Ethane-Bridged Zinc Porphyrin Dimers in Langmuir−Shäfer Thin Films: Structural and Spectroscopic Properties

Ludovico Valli,*,† Serena Casilli,† Livia Giotta,† Bruno Pignataro,‡ Sabrina Conoci,§ Victor V. Borovkov,|| Yoshihisa Inoue,|| and Salvatore Sortino*,⊥

Dipartimento di Ingegneria dell'Innovazione, Università di Lecce, I-73100 Lecce, Italy, Dipartimento di Chimica Fisica "F. Accascina", Università di Palermo, I- 90128, Palermo, Italy, LoC R&D, Microfluidics Division, CPG Group, STMicroelectronics, I-95121 Catania, Italy, Entropy Control Project, ICORP, JST, Toyonaka 560-0085, Japan, and Dipartimento di Scienze Chimiche, Università di Catania, I-95125 Catania, Italy

Received: September 2, 2005; In Final Form: January 26, 2006

This work reports on the structural and spectroscopic properties of ethane-bridged Zn porphyrin dimers (**1**) in Langmuir−Schäfer (LS) thin films by combining scanning force microscopy (SFM) with film balance, UV−vis absorption, fluorescence, and nanosecond laser flash photolysis measurements. Results show that depending on the surface pressure the Langmuir films of pure **1** can be arranged in two different condensed phases, whereas SFM of the LS films shows characteristic fractal networks constituted by nanoscopic aggregates. The spectral findings agree with a picture in which **1** is apparently present in the anti conformation but aggregated in a sort of H-type structure whose optical features resemble those of the syn conformer. This type of structure is not responsive to light stimuli. By diluting **1** in arachidic acid the porphyrin aggregation is significantly minimized with **1** exhibiting almost exclusively the anti conformation. As a result the LS films become photoresponsive, showing fluorescence emission and triplet−triplet transient absorption.

Introduction

In the massively explored arena of porphyrins and their derivatives, covalently linked mono- and heterometalated porphyrin dimers have received special attention by interdisciplinary areas of the scientific community. This interest has been stimulated by reasons related to both fundamental aspects and practical purposes. In fact, these chromophoric systems represent effective models of photosynthetic electron transfer,[1] singlet or triplet energy transfer,[2] and interchromophore interactions[3] and are well-suited for a large variety of potential applications in many fields of technological interest spanning from photoconductors[4] to chemical sensors.[5] In addition, the conformational changes induced by the molecular surroundings in these chromophores are of paramount importance in real life processes[6] and may also provide insights into the field of molecular engineering and electronics.[7] In this context, some of us (V.V.B. and Y.I.) have extensively investigated the conformational changes of the symmetrical ethane-bridged bis(Zn porphyrin) (**1**) in solution phase[8] (Scheme 1).

The results that emerged from these studies showed that **1** adopts a syn conformation at room temperature in a variety of noncoordinating solvents and that this conformation does not break apart, even upon dramatic temperature changes. However, the presence of either alcohols or amines encourages the shift of the conformational equilibrium toward the anti conformer upon temperature decrease or even at room temperature in the case of external ligands with high binding affinity. The mechanism of this unprecedented phenomenon is based on the enhanced alcohol ligation to Zn porphyrin at low temperature (or amine at room temperature), which is capable of destroying the strong $\pi-\pi$ inter-porphyrin interactions (Scheme 1). Interestingly, this conformational switching is accompanied by a significant change in the optical properties of **1**. In particular, the Soret band increases in intensity and its absorption maximum shifts from 397 to 420 nm upon syn−anti conversion.[8]

SCHEME 1: Molecular Structure (top) and Syn ⇄ Anti Conformational Equilibrium for the Investigated Ethane-Bridged Bis(Zn porphyrin) (1)

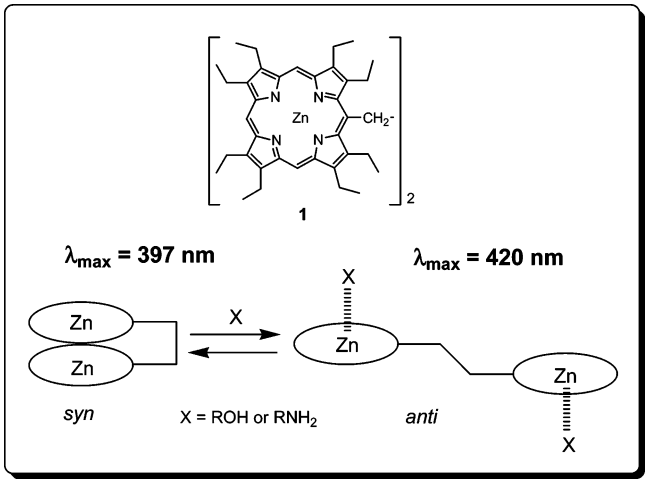

In our recent work we shed light on the behavior of floating films of **1** at the air−water interface, proving for the first time that the syn−anti conformational transition can be encouraged by the ligation of suitable amphiphiles, such as *n*-octadecylamine and arachidic acid, even at the liquid−air interface.[9] Beyond contributing to the comprehension of the two-dimensional arrangement of the dimer at the water surface, this study can

* Corresponding authors. E-mail: ludovico.valli@unile.it; ssortino@unict.it
† Università di Lecce.
‡ Università di Palermo.
§ STMicroelectronics.
|| Entropy Control Project.
⊥ Università di Catania.

10.1021/jp054974v CCC: $33.50
Published on Web 02/23/2006

be helpful for the achievement of three-dimensional multilayers on solid substrates characterized by a specific organization of the chromogenic units. In this regard it should be stressed that controlling and changing the orientation of porphyrins in nanolayers is a key issue both for fundamental physicochemical aspects and in the perspective of developing photonic and electronic devices, which require transport of excitons or charge carrier.[10]

Among the wide range of approaches to construct porphyrin arrays, the Langmur−Blodgett (LB) technique is one of the most widely exploited by virtue of its general applicability in fabricating highly ordered film structures with controlled orientation at the molecular level.[11] In the case of porphyrins without any modification, this is, however, a difficult task due to their strong tendency for aggregation.[12] Nevertheless, many investigations have demonstrated that it is possible to obtain stable and rigid LB films of porphyrins with controlled orientation by incorporating diluent molecules, such as ionic and nonionic surfactants, into LB films.[13]

The present work reports on the fabrication of multilayer films of **1** alone and in a mixture with arachidic acid through a modification of the LB technique, the horizontal lifting or Langmuir−Schäfer (LS) method, and inspection of the molecular arrangement of the porphyrin dimer in the films by combining scanning probe microscopy with UV−vis absorption, fluorescence, and laser flash photolysis measurements. The structural properties of the **1** molecules are correlated with their response to light stimuli.

Experimental Section

Chemicals. Compound **1** was synthesized according to the previously reported method.[14] Arachidic acid, 1,1,1,3,3,3-hexamethyldisilazane, and pyridine (Sigma-Aldrich) were used as received. All solvents used (from Carlo Erba) were spectrophotometric grade.

Langmuir Experiments. Solid supported films of **1** were deposited by a KSV 5000 System 3 LB apparatus (850 cm^2). During the experiments, after each run, the trough was carefully washed with chloroform, acetone, ethanol, and water. Ultrapure water (Millipore Milli-Q, 18.2 MΩ cm) was used as the subphase. The temperature of the subphase was regulated at 20 °C by a Haake GH-D8 apparatus. **1** was dissolved in $CHCl_3$ at a concentration of 1.2×10^{-4} M. A 400 μL amount of **1** solution was spread by a gastight syringe onto the subphase, adding small drops at different locations on the water. After the solvent evaporated, the floating film at the air−water interface was compressed continuously at a speed of 10 mm m^{-1}. The surface pressure was simultaneously monitored by a Wilhelmy balance while obtaining an isotherm of the sample. The surface layer was transferred by the Langmuir−Shaefer (LS) deposition technique, which is performed by lowering the substrate horizontally until contact with the floating film. During the transfer we typically used surface pressures of 16 and 30 mN/m. Deposition was carried out on clean quartz (for the spectroscopic measurements) or silicon oxide (for the morphological measurements) slides (30×40 mm^2). Prior to the transfer both substrates were hydrophobized by exposure for 24 h to a saturated atmosphere of 1,1,1,3,3,3-hexamethyldisilazane (HMDS).

Scanning Force Microscopy (SFM). SFM analysis was carried out in air using a Multimode/Nanoscope IIIa equipped with an extender electronics module (Digital Instruments) in tapping mode. Commercially available tapping etched silicon probes (Digital) with a pyramidal shape tip having a nominal curvature of 10 nm and a nominal internal angle of 35° were used. During the analysis the cantilever, about 125 μm long, with a nominal spring constant of 20−100 N/m, oscillated at its resonance frequency of about 300 kHz. Height and phase images were recorded contemporaneously by collecting 512×512 points for each scan and maintaining the scan rate below 1 Hz.

Steady-State Absorption and Emission Spectroscopy. Absorption and fluorescence spectra were recorded with a Beckman 650 DU spectrophotometer and a Spex Fluorolog-2 (model F-111) spectrofluorimeter, respectively. The fluorescence spectra of the LS films were recorded aligning the quartz slides at an angle of 30°/60° (excitation/emission) using a slide holder specially designed and were corrected by background light scattering using a blank slide. Reflection of the excitation from the quartz was to the opposite side of the emission detection.

Laser Flash Photolysis Setup. All samples were excited with the second harmonic of a Nd:YAG Continuum Surelite II-10 laser (532 nm, 6 ns, ∼10 mJ). The quartz plate with the LS films was aligned at an angle of 45° with respect to both the excitation and the monitoring beams. The reflection of the excitation from the quartz plate was to the opposite side of the transient signal detection. The measurements in solution were carried out with a 10×10 mm^2 quartz cell with a 3 mL capacity. In both cases, the excited samples were analyzed with a Luzchem Research mLFP-111 apparatus with an orthogonal pump/probe configuration. The probe source was a ceramic xenon lamp coupled to quartz fiber-optical cables. The laser pulse and the mLFP-111 system were synchronized by a Tektronix TDS 3032 digitizer, operating in pretrigger mode. The signals from a compact Hamamatsu photomultiplier were initially captured by the digitizer and then transferred to a personal computer, controlled by Luzchem Research software operating in the National Instruments LabView 5.1 environment. The sample temperature was 295 ± 2 K. The energy of the laser pulse was measured at each shot with a SPHD25 Scientech pyroelectric meter.

Results and Discussion

LS Films of Pure 1. Figure 1 presents the surface pressure vs area isotherm ($T = 20$ °C) of pure **1** spread at the air/water interface. It shows the presence of an expanded phase ($\Pi < 1$ mN/m) at areas per molecule larger than 140 $Å^2$. By increasing the pressure ($\Pi > 5$ mN/m) two steep regions indicating the formation of two different condensed phases are observed. The two steep features are separated by a kink at about 27 $Å^2$. By extrapolating the steep lines at zero pressure, we measured the limiting area per molecule ($A_\Pi \rightarrow 0$) of the two condensed phases resulting about 110 and 55 $Å^2$, respectively. The difference in $A_\Pi \rightarrow 0$ cannot be completely ascribed to an anti-syn switching upon compression. Indeed, these values are significantly smaller than those expected for the anti (160 $Å^2$) and syn (80 $Å^2$) conformers in a densely packed arrangement, as evaluated through computational methods (space-filling molecular models and Cerius2 software). This fact can be explained by considering that under the barrier compression part of the molecule escape out of the air/water plane gives rise to 3D growth (see below SFM data).

To deeply investigate the structural features of **1** in the condensed phase, we performed SFM measurements on freshly prepared solid supported thin films. These films were prepared by transferring through the LS technique the floating molecules on hydrophobized silicon substrates (see Experimental Section). Thin films of increasing thickness were fabricated by increasing the number of transfer runs accomplished at ambient temperature

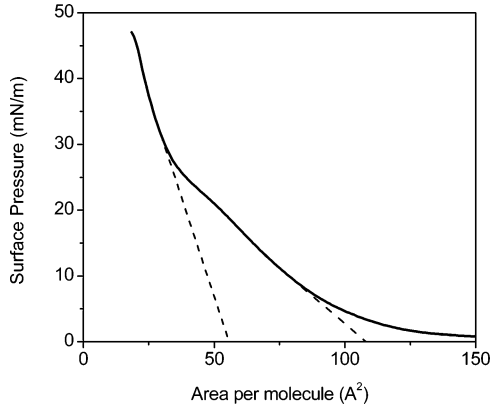

Figure 1. Isotherm of **1** in chloroform at 20 °C.

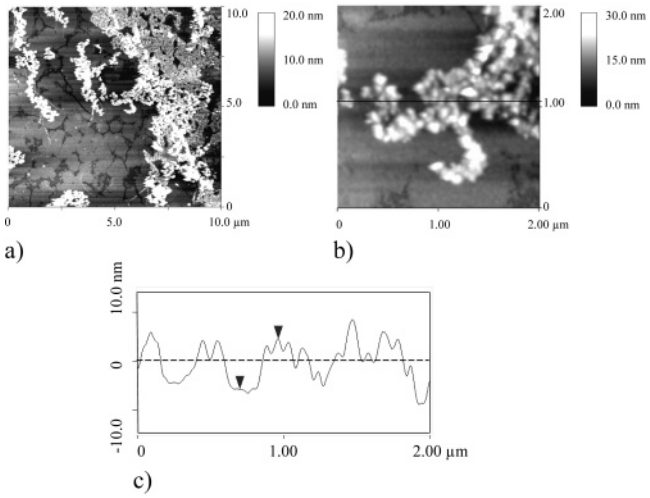

Figure 2. SFM investigation of LS film of **1** transferred on hydrophobized silicon by one run at 30 mN/m. (a) 2D 10 × 10 μm image; (b) zoom in peculiar region of a; (c) section analysis along the line marked in b. It can be inferred that the association of molecules within the nanoscopic ellipsoidal clusters is connected with the stronger interaction under compression between the **1** molecules than the **1**−water interaction.

with surface pressures of 16 and 30 mN/m. These two values of pressure have been chosen since each of them falls within one of the two different condensed phases observed within the isotherm in Figure 1.

Figure 2 shows the SFM investigation of **1** LS films transferred by a single transfer run at 30 mN/m. In particular, Figure 2a reports a 10 μm × 10 μm 2D image showing a branched molecular network characterized by a high degree of randomness. This kind of feature has been previously observed on larger (100 μm × 100 μm) length scales for the Langmuir film at the air/water interface by Brewster angle microscopy.[9] The film has mainly a bidimensional character with a basic layer about 5−10 nm thick. Note that there are different regions in which the film also extends three dimensionally with peaks which can be more than 15 nm tall. To understand in more detail the organization of **1** molecules within the film, we obtained images at different magnification. Figure 2b reports a zoom performed in a region of Figure 2a.

As a first observation it can be noted that the above dendritic open structures with a high degree of branching arise from the aggregation of ellipsoidal organic nanoparticles 5−10 nm thick and 20−70 nm wide (see also section analysis in Figure 2c). Due to the nanoscopic dimension of these particles, the measured lateral size is expected to be significantly affected by the well-known SFM tip/sample convolution broadening effect,[15] and as a consequence the above value has to be considered as overestimated. In particular, according to the model proposed by García et al.,[15] we evaluate that the real size, imaged by a tip 10 nm in radius, of an ellipsoidal particle 40 nm width and 10 nm tall is about 16 nm. The volume of a particle with these dimensions is about 1000 nm^3. By considering that the **1** molecule, for instance, in the anti conformation has a volume of ca. 100 Å^3, the above estimated particle dimensions are in agreement with a picture in which the ellipsoidal nanostructures arise from the aggregation of thousands of **1** molecules. The highest peaks of the film arise from the overstaking of particles leading to a 3D growth of the film. The aggregation in 3D particles which somewhere overstake each other can explain the above hypothesis concerning the escape of molecules from the Langmuir film plane.

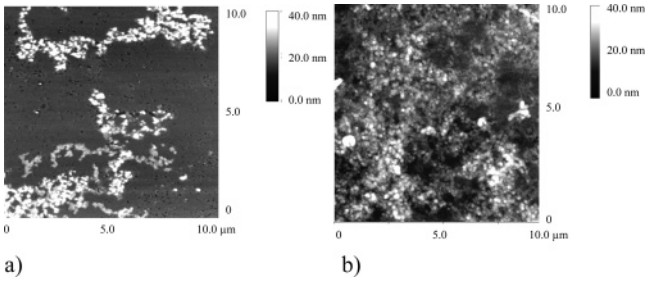

Figure 3. SFM investigation of LS film of **1** transferred on hydrophobized silicon by 1 run (a) and 16 runs (b) at 16 mN/m.

As a second important finding, it can be noted that branched features are present also at this smaller length scale. As above recalled, the imaged SFM branched features closely resemble those previously observed by Brewster angle microscopy at the air/water interface.[9] This finding further corroborates the fact that the molecular association is not induced by the transfer process but is expected to be prevalently originated at the air−water interface under the barrier compression. The formation of branches in thin solid films might be expected to be induced by a spinodal dewetting process.[16] However, in our sample this mechanism should not be evoked since the coupling between the Brewster angle and the SFM images indicates that there is no important influence of the transfer process on the morphology of the resulting thin layer.

Due to the branched organization the substrate surface is not completely covered and a significant part of the substrate with its hydrophobic layer can be freely visualized by SFM.

From a morphological point of view, the pressure of 30 mN/m leads to branches more densely interconnected and packed with respect to those observed at 16 mN/m (Figure 3a). On the other hand, the average film height of about 10 nm at 30 mN/m is not significantly different from that observed at 16 mN/m. These findings corroborate the fact that in this range of pressures the barrier compression mainly induces the lateral aggregation of molecules, rather than their 3D overstacking.

According to the above scenario, by assuming that in our sample the mesoscale morphology observed by SFM is originated at the air−water interface and the resulting structures are transferred to the solid surface without significant disturbance, the observed branches might be more likely explained in terms of a fractals model like the cluster−cluster aggregation or diffusion-limited aggregation (DLA) ones.[17] In particular, the DLA model assumes that the particles originate far away from the immobile developing structure and perform a random walk once they encounter the structure and stick to it. Quantitatively,

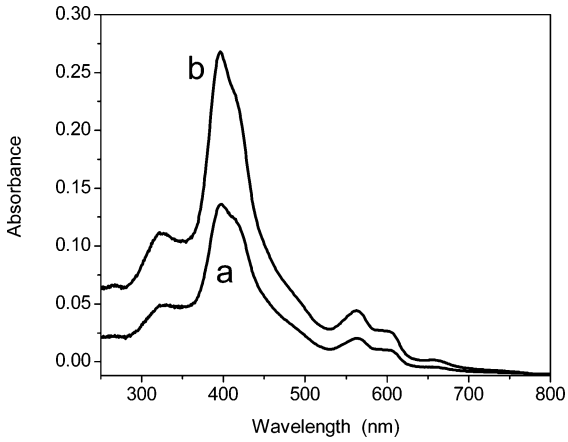

Figure 4. UV−vis absorption spectra of 12 layers of LS films deposited at (a) 16 and (b) 30 mN/m.

the DLA model predicts branching self-similar structures with a fractal dimension *D* estimated to be around 1.67. On the other hand, the cluster−cluster aggregation model assumes that there is no unique seed or growth site and aggregation occurs at any location of the system. Moreover, the newly formed clusters can move randomly and stick to other clusters to form large aggregates. The fractal dimension *D* for that model is 1.38.

In our case the sample observed in Figure 2a shows a fractal dimension *D* around 1.68, whereas that obtained at lower pressures (Figure 3a) shows a fractal dimension *D* of about 1.5. Similar values for 2D cluster−cluster DLAs have been reported by other authors.[18] Accordingly, low values of the fractal dimension ($D < 1.5$) are indicative of a fast aggregation process with a high probability of cluster−cluster sticking and collision, whereas higher values ($D > 1.5$) correspond to a slow aggregation process with low probability of sticking providing more compact structure of the aggregates.

To obtain full coverage more than four runs have to be performed. The increase of the number of layers transferred is accompanied as expected by a progressive increase of the roughness. Quantitatively, the root-mean-square roughness (RMS) of the films transferred at 30 mN/m increases from about 5 to 9.5 nm and up to 22 nm for 1, 4, and 12 layers, respectively. For a pressure of 16 mN/m the RMS increases from about 5 to 8 and up to 12.5 nm for 1, 4, and 12 layers, respectively. These RMS data have been evaluated by off-line analysis of SFM images 100 μm^2 in size. For the thicker films it is evident that the higher the pressure used during the transfer, the larger the roughness. The general feature arising from these data and the SFM images (data not shown) is that the transfer of several layers causes a disordered 3D stacking of the nanoscopic aggregates of **1** molecules.

Although the above data give us direct information on the mesoscopic and nanoscopic 2D and 3D arrangement of **1** molecules, a very intriguing point consists of the understanding of how the individual molecules assemble within each nanoaggregate and which of their possible conformations (syn or anti) they on average assume. This point has been explored by spectroscopic measurements. Figure 4 shows the UV-vis absorption spectra related to 12 layers of **1** transferred at pressures of 16 and 30 mN/m. The presence of the 395 and 420 nm components in the Soret region would appear, in principle, to be consistent with the presence of the syn and anti conformers, respectively.

It can be seen that the absorption exhibited in the whole range of wavelengths by the layers transferred at higher pressure is almost 2-fold that of the films obtained at lower pressure.

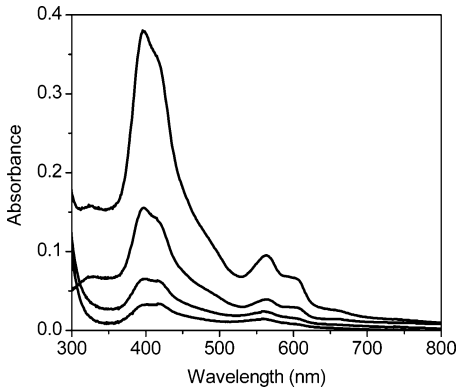

Figure 5. UV-vis absorption spectra of LS film containing 2, 4, 12, and 24 layers (from bottom to top) of **1** deposited at 16 mN/m.

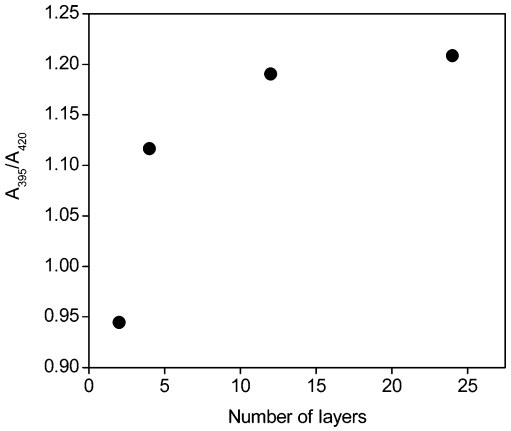

Figure 6. Absorbance ratio 395/420 nm as a function of the number of layers.

However, it should also be noted that both spectra are similarly shaped. This seems to be in agreement with the above proposal that no anti−syn conformational change of **1** occurs as the deposition pressure increases (vide supra). Rather, the 2-fold enhancement in the absorbance value should be connected to the above observed increase in density with pressure, which in turn allows the transfer of a higher amount of molecules per run on the substrate. At this stage we cannot exclude that this phenomenon is accompanied by a partial molecular reorientation as it has been observed by other authors that a molecular tilt can be induced by pressure.[13b] This fact might explain the change in slope at 27 mN/m in the above Langmuir isotherm, leading to the formation of two different condensed phases.

More insights into the arrangement of the porphyrin chromophores in the LS films are gained by the UV-vis absorption spectra of LS films containing a different number of layers deposited at 16 mN/m. Figure 5 shows that the shape of the Soret band is strictly dependent on the number of LS layers and that the increase of the absorbance as a function of the latter does not follow a linear behavior.

In particular, the plot reporting the ratio of the absorbance values at key wavelengths 395 and 420 nm as a function of the number of layers (Figure 6) provides better perceptible evidence for a more dominating contribution at 395 nm over that at 420 nm with increasing number of layers.

A probable arrangement model of **1** in the LS films, consistent with the results presented above, is sketched in Scheme 2.

It might be envisaged that molecules of **1** are preferentially present in the anti conformation according to what was demonstrated for floating films,[9] but they are organized in sort of H-type aggregates, where the upper porphyrin of the first

SCHEME 2: Probable Arrangement of 1 in a Single Layer of the LS Films

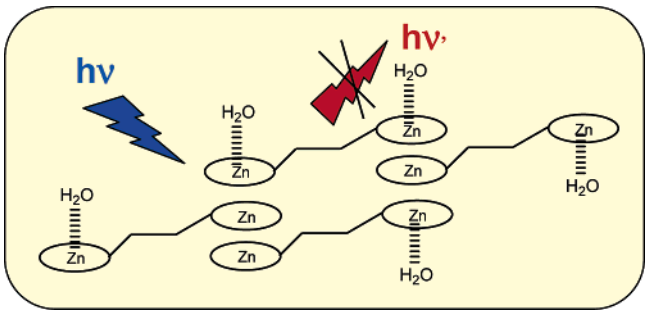

molecule is sitting above the lower porphyrin of the second molecule. Therefore, the UV-vis absorption spectrum shows the concomitant appearance of blue- and red-shifted transitions (395 and 420 nm) in the Soret region. Additionally, the observed nonlinear dependence of the absorption from the number of layers could suggest that the increase of the blue-shifted transition may reflect a parallel increase of the H-type aggregates. However, we cannot exclude the possibility that upon increasing the number of layers the anti form turns back to the syn form due to the increasing hydrophobic environment inside the films, thus forcing the external water ligands to dissociate and leave the Zn central ions.

To investigate the response to light stimuli of the above films, we carried out fluorescence and nanosecond laser flash photolysis measurements. In fact, in contrast to what was observed in solution, **1** is not responsive to light stimuli when incorporated in the LS films. Indeed, neither significant fluorescence nor detectable transient absorption was detected upon light excitation of films of **1** containing 24, 48, or 96 LS layers. This might be due to effective, quite common quenching processes in the porphyrin aggregates that govern the fate of the excited chromophores in the closed-packed LS structure.[13b] To ascertain if the quenching is a result of either an intra- or an interlayer mechanism, we prepared LS films consisting of a layer of **1** interspaced with two layers of arachidic acid (AA). As ideally illustrated in the inset of Figure 7, such a strategy should preclude the interlayer communication between the chromophores. The absorption features of these LS films (see Figure 7) are basically the same to those observed in the absence of the interlayer spacer (see Figure 5 for comparison), exhibiting both the 395 and 420 nm components in the Soret absorption region. However, neither significant fluorescence nor transient signals are observed. On the basis of these findings the insensitivity of **1** to light excitation cannot be ascribed to the porphyrin overstacking but, more likely, is a result of efficient quenching processes taking place within every single layer.

The model proposed above in Scheme 2 also provides an explanation for the lack of fluorescence observed in the films. In fact, it is well known that superposed H aggregates are nonemissive as a result of the forbidden transition from the fluorescent S_1 state.[19]

LS Films of 1 in a Mixture with Arachidic Acid. The use of porphyrins in conjunction with amphiphilic compounds, such as ionic and nonionic surfactants, represents a well-suited strategy for controlling the molecular orientation, aggregation, and other structural features of porphyrins.[13b,20] With this in mind, we co-spread **1** and AA in a molar ratio of 1:30. In our previous investigation we demonstrated that the floating films obtained under these experimental conditions are characterized by almost isolated molecules of **1** with the arachidic acid acting not only as a spacer but also as a weak ligand for the Zn centers

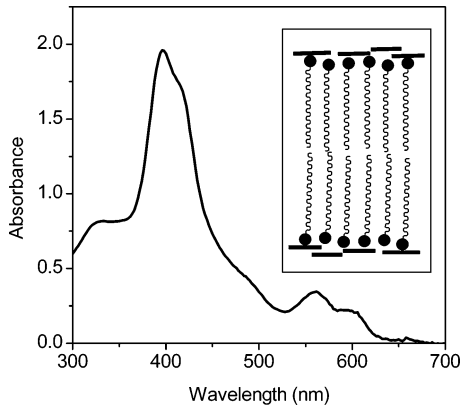

Figure 7. UV-vis absorption spectrum related to 73 layers of **1** and 150 layers of AA. Each layer of **1** is interspaced by two layers of AA as ideally reported in the inset.

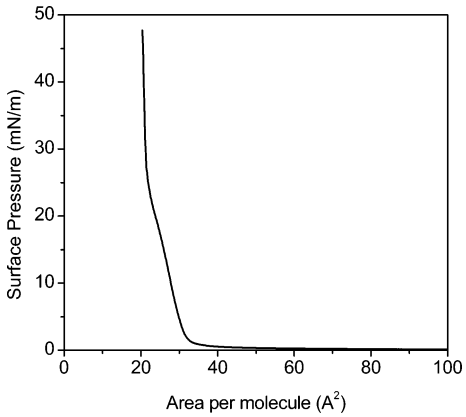

Figure 8. Isotherm for the system formed by **1** and arachidic acid at the molar ratio 1:30, co-spread from chloroform at 20 °C.

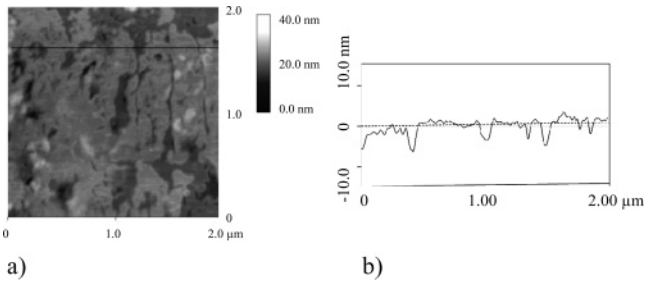

Figure 9. SFM investigation of mixed LS film obtained by transferring 16 layers of **1**:AA 1:30 on hydrophobized silicon: (a) 2D 2 × 2 μm image; (b) section analysis along the line marked in a.

of the porphyrins.[9] The corresponding Π vs *A* curve in Figure 8 is in accordance with such observations; in fact, the value of 22 Å^2/molecule of the limiting area per molecule of arachidic acid in the mixture with **1**, where the fatty acid is in large excess compared to the bis-porphyrin derivative, is close to the well-known value of 20 Å^2/molecule for the pure arachidic acid. Mixed LS films were thus prepared and inspected by SFM and spectroscopic techniques.

SFM was used to gather inside the miscibility or phase separation of the component molecules in the mixed LS films. In fact, generally two scenarios are possible when two types of molecules are mixed. One is that two-component hybrids form a homogeneous monolayer with preferable mutual miscibility. The other is that two molecules are immiscible and form separated phases or domains which can be directly imaged by SFM. Figure 9 shows SFM images of the mixed LS films (16 layers) on silicon surfaces.

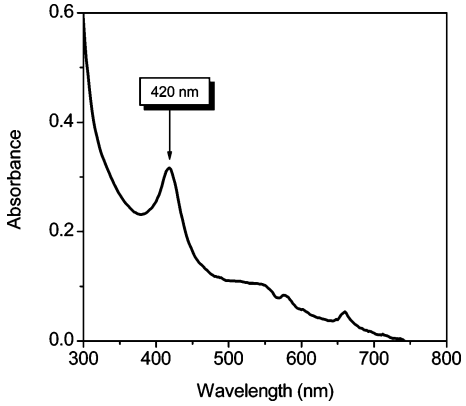

Figure 10. UV-vis absorption spectrum of mixed LS films obtained by transferring 80 layers of **1**:AA (1:30).

This image shows the typical appearance of pure arachidic acid based LS films with the characteristic layer-by-layer conformation, uniformity, and flatness.[21]

In particular, the section analysis in Figure 9b shows the characteristic layer flatness and layer-to-layer distance (about 3 nm) of AA LS films indicating that in the mixed film the AA molecules are oriented almost perpendicularly to the substrate with only a slight tilting. Moreover, no branched networks characteristic of the **1** aggregation are observed. This finding together with the flatness of each layer indicate that molecules of **1** are well-dissolved within the amphiphilic matrix without drastically disturbing the intermolecular arrangement of AA molecules, the porphyrin−porphyrin interaction being drastically minimized.

Spectroscopic measurements allow obtaining decisive information to disclose the arrangement of **1** under these experimental conditions. Figure 10 shows the UV-vis absorption spectrum of a representative mixed LS film. It is well evident that, in contrast to what was observed for the LS films of pure **1**, the Soret absorption consists of a single, well-defined band with a maximum at 420 nm analogously to what was expected for the pure anti conformer.

Interestingly, these mixed LS multilayers are photoresponsive. Actually we obtained a fluorescence spectrum characterized by two well-defined bands with maxima at ca. 607 and ca. 670 nm (Figure 11a).

Analogously to the absorption, the emission features also contain information supporting the presence of the anti conformer of **1** in the films. This is proven by comparing the fluorescence spectrum of the film with those of **1** in toluene solution in the absence and presence of a large excess of pyridine (Figure 11b). This species is a well-known complexing agent for Zn porphyrins,[22] and in the case of compound **1** it is able to trigger syn−anti switching even at room temperature due to the effective binding constant with the metal centers.[23] In fact, as illustrated in Figure 11b the emission of **1**, present as the syn conformer in this solvent, consists of a main band at ca. 620 nm and a shoulder at longer wavelengths. Addition of pyridine destroys the strong $\pi-\pi$ inter-porphyrin interactions and results in a significant change in the fluorescence spectrum which is characterized by two well-defined emission bands with maxima at 607 and 660 nm, in very good agreement with the emission exhibited by the mixed LS films.

The reduction of the intralayer quenching effects also allows observing transient absorption signals upon laser excitation of the mixed LS films. Figure 12a shows the transient spectra recorded at different delay times with respect to the laser pulse. The spectrum taken at 1 μs is characterized by absorption

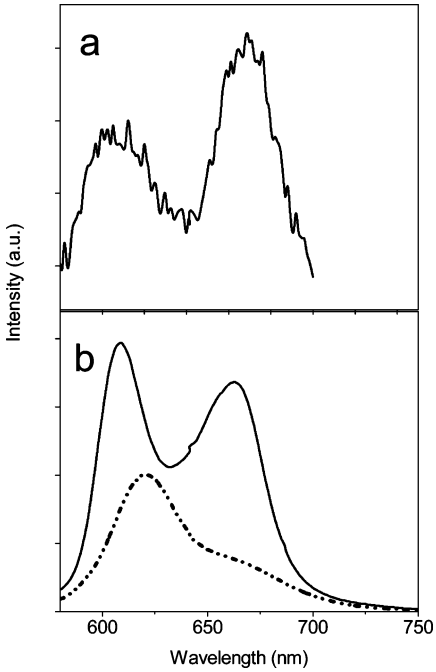

Figure 11. (a) Fluorescence spectrum of mixed LS films obtained by transferring 80 layers of **1**:AA (1:30). (b) Fluorescence spectra of **1** (2×10^{-6} M) in toluene solution in the absence (dashed line) and presence (solid line) of pyridine (10^{-2} M) a room temperature.

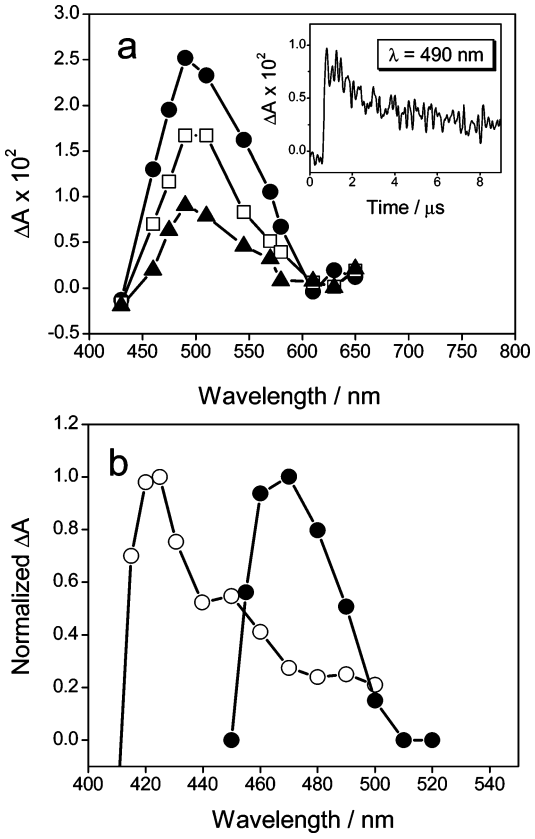

Figure 12. (a) Transient absorption spectra observed (●) 1, (□) 2, and (▲) 8 μs after 532 nm laser excitation of mixed LS films obtained by transferring 80 layers of **1**:AA (1:30). (b) Transient absorption spectra observed 0.5 ms after 532 nm laser excitation of a toluene solution of **1** (10^{-5} M) (○) in the absence and (●) presence of pyridine (0.1 M) at room temperature.

maximum at ca. 490 nm. The decay of this species is independent of the wavelength, and no new transient is generated

SCHEME 3: Proposed Scheme for the Arrangement of the Mixed LS Films

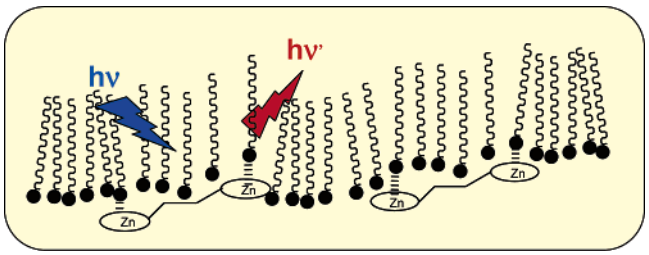

concurrently. The kinetic profile (inset, Figure 12a) is fitted fairly well by a monoexponential analysis, affording a first-order rate constant $k_1 = 1.6 \times 10^5\ s^{-1}$ in accordance with a quite homogeneous distribution of the chromophores within the film.

The transient observed can be assigned to the lowest excited triplet state of **1** in the anti form on the basis of comparative laser flash photolysis experiments carried out in toluene solutions of **1** in the absence and presence of a large excess of pyridine (Figure 12b). According to literature[19] the triplet absorption maximum of **1** in toluene (where **1** exists as the syn conformer) shows a maximum at 420 nm and a shoulder at ca. 450 nm. On the other hand, the triplet spectrum observed in the presence of the base exhibits a maximum at ca. 470 nm and a different spectral shape.[24] These characteristics are very comparable to those exhibited by the mixed LS films and corroborate the existence of **1** almost exclusively as nonaggregate anti conformer in the film.

A schematic model illustrating the arrangement of **1** in the mixed LS films according to the overall presented results is depicted in Scheme 3.

Conclusions

In this paper we gained interesting insight into the self-organization of a porphyrin dimer in multilayer thin films and the related photophysical properties by combining scanning force microscopy with film balance, UV−vis absorption, fluorescencev and nanosecond laser flash photolysis measurements. The arrangement of the chromophores in LS condensed thin films leads to different scenarios depending on the experimental conditions used (surface pressure, molecular environment, etc.). The pure film of **1** shows a characteristic fractal structure consisting of randomly assembled nanoscopic aggregates that can be interpreted in terms of cluster−cluster and DLA mechanisms. The spectroscopic results indicate that within each nanoparticle **1** is probably arranged in a sort of H-type structure characterized by a Soret absorption typical for the *apparent* presence of both the syn and the anti conformers. This type of structure makes the film unresponsive to light stimuli as a result of the effective intralayer self-quenching processes, the forbidden transition from the S_1 state (typical for superposed porphyrin H aggregates), or both.

Introduction of the surfactant has profound effects on the morphological and spectroscopic properties of the related mixed LS films. Indeed, more homogeneous LS films in which the porphyrin aggregation is efficiently suppressed are obtained. In contrast to those of pure **1**, in this mixed LS solid supported thin film the porphyrins arrange almost exclusively in the anti conformation. This is attributable to the double role of the arachidic acid which acts both as a spacer and a weakly coordinating agent. As a result, these multilayers become photoresponsive, exhibiting fluorescence emission and triplet−triplet transient absorption. On the basis of the work presented herein and by taking into account the results recently obtained by some of us on the supramolecular chirogenesis in the ethane-bridged bis(zinc porphyrin),[8c−e,25] we consider that the fabrication of mixed LS films of **1** with chiral surfactants may represent a further intriguing research goal to pursue.

Acknowledgment. We thank the MIUR (FIRB research projects, Rome, Italy) for financial support. We are also grateful to Mr. Luigi Dimo for his inestimable help in the LS procedures. Consorzio Catania Ricerche is acknowledged for hospitality in his laboratory.

References and Notes

(1) (a) Okamoto, K.; Fukuzumi, S. *J. Am. Chem. Soc.* **2003**, *125*, 12416. (b) Gust, D.; Moore, T. A.; Moore, A. L.; Leggett, L.; Lin, S.; DeGraziano, J. M.; Hermant, R. M.; Nicodem, D.; Craig, P.; Seely, G. R.; Nieman, R. A. *J. Phys. Chem.* **1993**, *97*, 7926.

(2) (a) Splan, K. E.; Keefe, M. H.; Massari, A. M.; Walters, K. A.; Hupp, J. T. *Inorg. Chem.* **2002**, *41*, 619. (b) Andrèasson, J.; Kajanus, J.; Martensson, J.; Albisson, B. *J. Am. Chem. Soc.* **2000**, *122*, 9844.

(3) Jiang, B.; Yang, S.; Jones, E. W., Jr. *Chem. Mater.* **1997**, *9*, 2031

(4) (a) Splan, K. E.; Massari, A. M.; Hupp, J. T. *J. Phys. Chem. B* **2004**, *108*, 4111. (b) Hasobe, T.; Imahori, H.; Yamada, H.; Sato, Y.; Ohkubo, K.; Fukuzumi, S. *Nano Lett.* **2003**, *3*, 409.

(5) (a) Yagi, S.; Ezoe, M.; Yonekura, I.; Takagishi, T.; Nakazumi, H. *J. Am. Chem. Soc.* **2003,** *125*, 4068. (b) Tepore, A.; Serra, A.; Arnold, D. P.; Manno, D.; Micocci, G.; Genga, A.; Valli, L. *Langmuir* **2001**, *17*, 8139.

(6) (a) Casella, L.; Colonna, S. In *Metalloporphyrins Catalized Oxidations;* Montanari, F., Casella, L., Eds.; Kluwer Academic Publisher: Dordrecht, 1994; p 307. (b) Gentemann, S.; Medforth, C. J.; Forsyth, T. P.; Nurco, D. J.; Smith, K. M.; Fajer, J.; Holten, D. *J. Am. Chem. Soc.* **1994**, *116*, 7363.

(7) (a) Ambroise, A.; Wagner, R. W.; Rao, P. D.; Riggs, J. A.; Hascoat, P.; Diers, J. R.; Seth, J.; Lammi, R. K.; Bocian, D. F.; Holten, D.; Lindsey, J. S. *Chem. Mater.* **2001**, *13*, 1023. (b) Burrell, A. K.; Officer, D. L.; Reid, W. D. C.; Wild, K. Y. *Angew. Chem., Int. Ed. Engl.* **1998**, *37*, 114. (c) Arnold, D. P.; Borovkov, V. V.; Ponomarev, G. V. *Chem. Lett.* **1996**, 485. (d) Iseki, Y.; Inoue, S. *J. Chem. Soc., Chem. Commun*. **1994**, 2577.

(8) (a) Borovkov, V. V.; Lintuluoto, J. M.; Inoue, Y. *J. Phys. Chem. B* **1999**, *103*, 5151. (b) Borovkov, V. V.; Lintuluoto, J. M.; Inoue, Y. *Tetrahedron Lett.* **1999**, *40*, 5051. (c) Borovkov, V. V.; Lintuluoto, J. M.; Fujiki, M.; Inoue, Y. *J. Am. Chem. Soc.* **2000**, *122*, 4403. (d) Borovkov, V. V.; Lintuluoto, J. M.; Inoue, Y. *J. Phys. Chem. A* **2000**, *104*, 9213. (e) Borovkov, V. V.; Hembury, G. A.; Yamamoto, N.; Inoue, Y. *J. Phys. Chem. A* **2003**, *107*, 8677.

(9) Borovkov, V. V.; Casilli, S.; Conoci, S.; Inoue, Y.; Sortino, S.; Valli, L. *Surf. Sci* **2004**, *572*, 66.

(10) (a) Donker, H.; Koehorst, R. B. M.; Schaafsma, T. J. *J. Phys. Chem. B* **2005**, *109*, 17031. (b) Donker, H.; van Hoek, A.; van Schaik, W.; Koehorst, R. B. M.; Yatskou, M. M.; Schaafsma, T. J. *J. Phys. Chem. B* **2005**, *109*, 17038. (c) Yokoyama, T.; Yokoyama, S.; Kamikado, T.; Mashiko, S. *J. Chem. Phys.* **2001**, *115*, 3014. (d) Hayashi, K.; Kawato, S.; Fujii, Y.; Horiuchi, T.; Matsushige, K. *Appl. Phys. Lett.* **1997**, *70*, 1384.

(11) (a) Ulman, A. *An Introduction of Ultrathin Organic Films From Langmuir−Blodgett to Self-Assembly*; Academic Press: New York, 1991. (b) Petty, M. C. *Langmuir−Blodgett film: an Introduction*; Cambridge University Press: Cambridge, 1996. (c) Liu, C. Y.; Pan, H. L.; Fox, M. A.; Bard, A. J. *Science* **1993**, *261*, 897. (d) Zasadzinski, J. A.; Viswanathan, R.; Madsen, L.; Garnaes, J.; Schwartz, D. K. *Science* **1994**, *263*, 1726. (e) Fendler, J. H.; Meldrum, F. C. *Adv. Mater.* **1995**, *7*, 607. Ulman, A. *Chem. Rev.* **1996**, *96*, 1533.

(12) (a) Jin, J.; Li, L. S.; Wang, X.; Li, Y.; Zhang, Y. J.; Chen, X.; Li, Y.-z.; Li, T. J. *Langmuir* **1999**, *15*, 6969. (b) Azumi, R.; Matsumoto, M.; Kuroda, S.-I.; King, L. G.; Crossley, M. J. *Langmuir* **1995**, *11*, 4056.

(13) (a) Anikin, M.; Tkachenko, N. V.; Lemmetyinen, H. *Langmuir* **1997**, *13*, 3002. (b) Viseu, M. I.; Goncalves da Silva, A. M.; Antunes, P.; Costa, S. M. B. *Langmuir* **2002**, *18*, 5772. (c) Efimov, A. V.; Anikin, M.; Tkachenko, N. V.; Mironov, A. F.; Lemmetyinen, H. *Chem. Phys. Lett.* **1998**, *289*, 572.

(14) Borovkov, V. V.; Lintuluoto, J. M.; Inoue, Y. *Helv. Chim. Acta* **1999**, *82*, 919.

(15) García, V. J.; Martinez, L.; Briceño-Valero, J. M.; Shilling, C. H. *Probe Microsc.* **1997**, *107*, 1.

(16) Warner, M. R. E.; Craster R. V.; Matar, O. K. *J. Colloid Interface Sci*. **2003**, *267*, 92.

(17) Grohens, Y.; Castelein, G.; Carriere, P.; Spevacek, J.; Schultz, J. *Langmuir* **2001**, *17*, 86.

(18) (a) Matsushita, M. In *The Fractal Approach to Heterogeneous Chemistry*; Avnir, D., Ed.; John Wiley and Sons Ltd.: New York, 1989. (b) Von Schulthess, G. K.; Benedek, G. B.; De Blois, R. W. *Macromolecules* **1980**, *13*, 939.

(19) McRae, E. G.; Kasha, M. *J. Chem. Phys.* **1958**, *28*, 271.

(20) Vandevyver, M.; Barraud, A.; Maillard Raudel-Teixer, P.; Gianotti, C. *J. Colloid Interface Sci.* **1982**, *85*, 571.

(21) Viswanathan, R.; Schwartz, D. K.; Garnaes, J.; Zasadzinski, J. A. N. *Langmuir* **1992**, *8*, 1603.

(22) (a) Kirksey, C. H.; Hambright, P.; Storm, C. B. *Inorg. Chem*. **1969**, *8*, 2141. (b) Gust, D.; Moore, T. A.; Moore, A. L.; Kang, H. K.; DeGraziano, J. M.; Liddell, P. A.; Seely, G. R. *J. Phys. Chem.* **1993**, *97*, 13637.

(23) Chernook, A. V.; Shulga, A. M.; Zenkevich, E. I.; Rempel, U.; von Borczyskowski, C. *J. Phys. Chem.* **1996**, *100*, 1918.

(24) Szintay, G.; Horváth, A. *Inorg. Chim. Acta* **2000**, *310*, 175.

(25) (a) Borovkov, V. V.; Lintuluoto, J. M.; Inoue, Y. *J. Am. Chem. Soc.* **2001**, *123*, 2979. (b) Borovkov, V. V.; Lintuluoto, J. M.; Inoue, Y. *Org. Lett.* **2000**, *2*, 1565. (c) Borovkov V. V.; Hembury G. A.; Inoue Y. *Angew. Chem., Int. Ed*. **2003**, *42*, 5310. (d) Borovkov, V. V.; Lintuluoto, J. M.; Sugeta, H.; Fujiki, M.; Arakawa, R.; Inoue, Y. *J. Am. Chem. Soc.* **2002**, *124*, 2993.